

Preparation of hierarchical flower-like γ -Al₂O₃@C composite exhibiting enhanced adsorption performance for Congo Red by high temperature transformation of γ -AlOOH@C precursors

Beibei Fang, Zepei Bao, Lun Lu, Lijun Zhao*, Huiyuan Wang*

Key Laboratory of Automobile Materials (Jilin University), Ministry of Education and School of Materials Science and Engineering, Jilin University, Changchun 130022, China

Fax: +86-0431-85095876

E-mail: lijunzhao@jlu.edu.cn

E-mail: wanghuiyuan@jlu.edu.cn

Experimental Section

1. Sample preparation

Aluminum nanopowders were purchased from Shanghai ChaoWei Nanotechnology Co., Ltd., hydrogen nitrate (HNO₃) and glucose were purchased from Beijing Chemicals Co. (Beijing, China). All chemicals were of analytical grade without further purification. In a typical experiment, Al nanopowders (0.2 g) were pretreated with 20 mL HNO₃ (0.1 M) via ultrasonication for 10 min. Then, the solution was centrifuged and washed three times with distilled water. The above pretreated Al nanopowders were re-dispersed into 40 mL glucose aqueous solutions (0.5 M), and followed by 30 min of ultrasonication (pH=6). After that, the mixture was transferred into a 50 mL of Teflon-lined stainless-steel autoclave, sealed, and maintained at 180 °C for 3 h before being cooled naturally. The precipitates were

centrifuged and washed several times with ethanol and deionized water, and then dried in a vacuum oven at 60 °C for 12 h to obtain γ -AlOOH@C precursors. Finally, the γ -AlOOH@C precursors were calcined at 600 °C at a heating rate of 3 °C /min and kept at 600 °C for 4 h under the protection of argon atmosphere to obtain γ -Al₂O₃@C composite.

As a comparison, pure γ -AlOOH and the corresponding calcinate (γ -Al₂O₃) were prepared with 40 mL of deionized water instead of 40 mL glucose aqueous solutions during the synthesis process while the other experimental parameters remained unchanged as before. Pure carbon sample was also prepared with 40 mL glucose aqueous solutions in the absence of Al powders followed by calcinations at 600 °C in Ar atmosphere, and other experimental parameters remained unchanged as before.

To investigate the influence of the temperature and reaction time on the morphology of the product, similar experiments were performed by varying temperature from 160 °C to 180 °C, and reaction times from 0.5 to 6.0 h at 180 °C, while the other conditions were kept the same as mentioned above.

2. Characterization

Structures and phases were identified by means of X-ray diffraction (XRD) with a Rigaku D/max 2500pc X-ray diffractometer with Cu K α radiation (λ) 1.54156 (Å) at a scan rate of 0.02°/1(s). Morphologies were characterized by a JEOL JSM-6700F field emission scanning electron microscopy (FESEM) operated at an acceleration voltage of 8.0 kV. Transmission electron microscopy (TEM) images, scanning TEM energy dispersive spectrometer (STEM-EDS) mappings were obtained

on a JEOL 2100F with an emission voltage of 200 kV. The specific surface areas of the as-prepared products were measured with Micromeritics ASAP 2020 Analyzer (USA) Brunauer-Emmet-Teller (BET) equipment by using nitrogen adsorption and desorption. The vibration property of γ -Al₂O₃@C was characterized by Raman spectroscopy T6400 with 514.5 nm excitation-beam wavelength. Thermogravimetric and differential thermal analyses (TG-DTA) were performed on an American Model TA SDT-Q600 analyzer at heating rate of range 10 °C /min and from room temperature to 600 °C under air or argon atmosphere.

3. Adsorption Experiments for CR.

Adsorption measurements for CR were performed by adding (under stirring conditions) 20 mg of as-prepared samples into 50 mL of Congo red (C₃₂H₂₂N₆O₆S₂Na₂) having a concentration of 100 mg/L at room temperature. Analytical samples were taken from the suspension after various adsorption times and separated by centrifugation. The CR concentrations were analyzed using a UV-vis spectrophotometer (UV-6100 PC, Shanghai, China).

The characteristic absorptions of CR around 500 nm were chosen to monitor the adsorption process, and adsorption capacity is calculated from the following mass balance equation:

$$Q_e = \frac{C_0 - C}{m}V$$

where Q_e (mg/g) is the amount adsorbed per gram of adsorbent at equilibrium, C_0 (mg/L) and C (mg/L) represent the initial concentration and concentration after

treatment, respectively, V (L) is the volume of the solution, and m (g) is the mass of the adsorbent used.

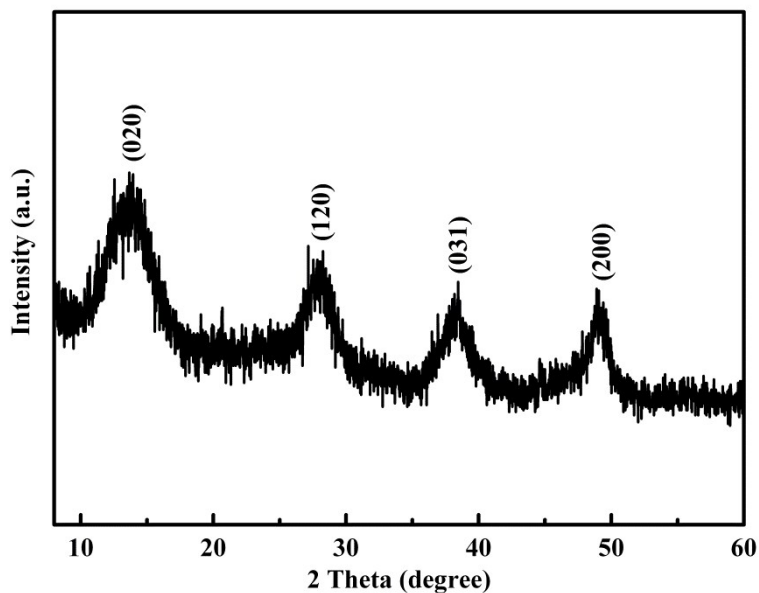


Figure S1 XRD pattern of the γ -AlOOH@C precursor prepared in the presence of glucose.

Figure S1 shows the XRD pattern of γ -AlOOH@C precursor sample. The observed diffraction peaks appear at 14.49, 28.18, 38.34 and 49.21 represent (020), (120), (031) and (002) reflections of γ -AlOOH, respectively, and all the mentioned above diffraction peaks are perfectly indexed to orthorhombic γ -AlOOH (JCPDS card No. 21-1307). While no obvious diffraction signals have been detected for the C phase, possibly due to the amorphous structure of carbon coating.

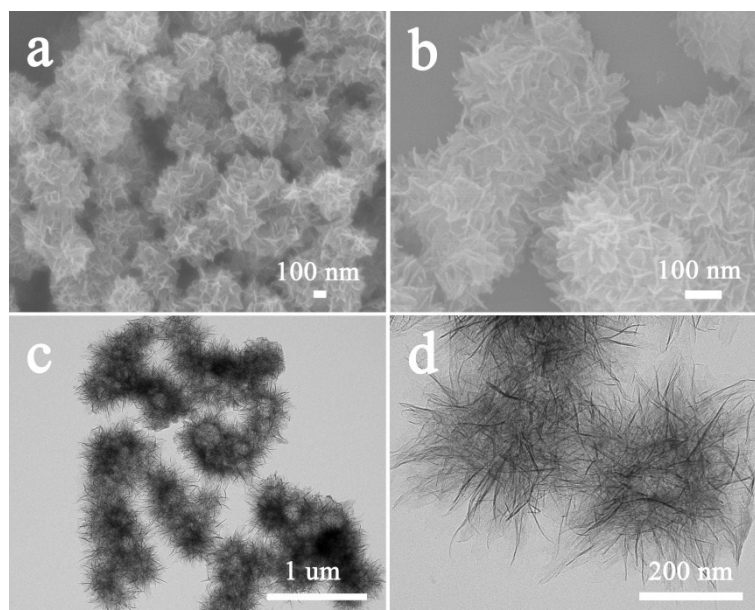


Figure S2 SEM (a, b) and TEM (c, d) images of γ -AlOOH@C precursor prepared in the presence of glucose.

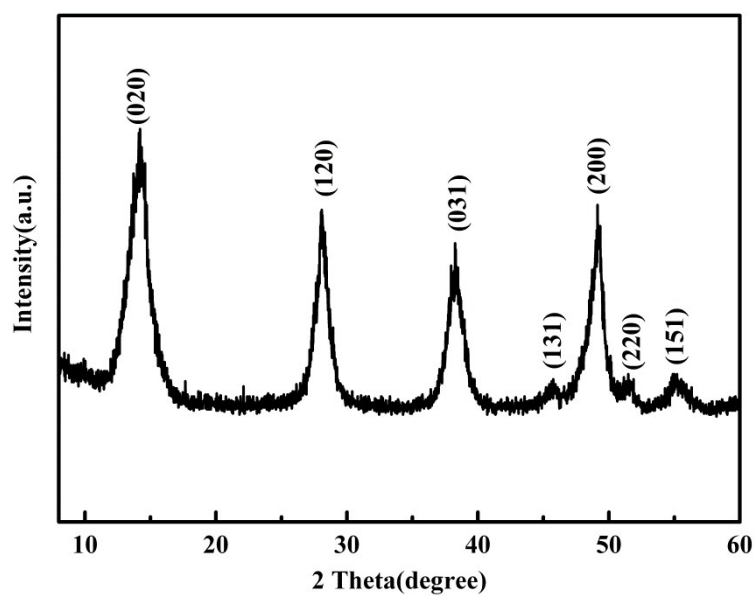


Figure S3 XRD pattern of γ -AlOOH precursor prepared in the absence of glucose.

The XRD pattern of precursor is shown in Figure S3, and all the diffraction peaks are perfectly indexed to orthorhombic γ -AlOOH (JCPDS card No. 21-1307).

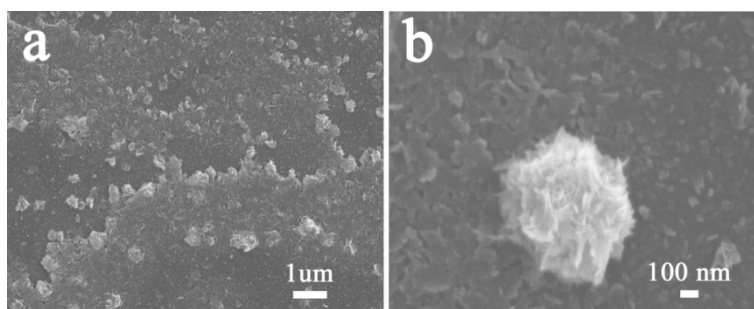


Figure S4 SEM images of γ -AlOOH precursor prepared in the absence of glucose.

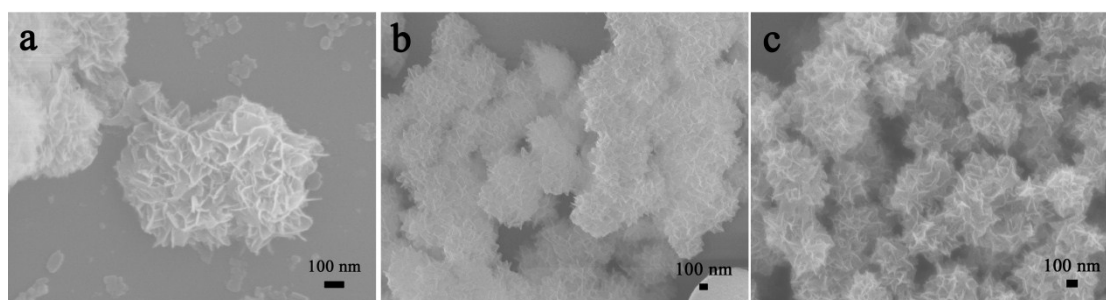


Figure S5 SEM images of γ -AlOOH@C precursor prepared at different heat treatment temperature a) 160 °C, b) 170 °C and c) 180 °C for 3 h. (other conditions: 0.2 g Al powders and 3.6 g glucose)

Figure S5 is the SEM images of γ -AlOOH@C precursor prepared at different heat treatment temperature. At 160 °C, lots of irregular sheets are presence besides flower-like structures. When the temperature was increased to 170 °C, flower-like structures with uniform morphologies were obtained, as shown in Figure S5b. However, some smooth carbon spheres also can be found. At 180 °C, it can be found that the γ -AlOOH@C precursor entirely consists of highly uniform flower-like structures without any free carbon spheres.

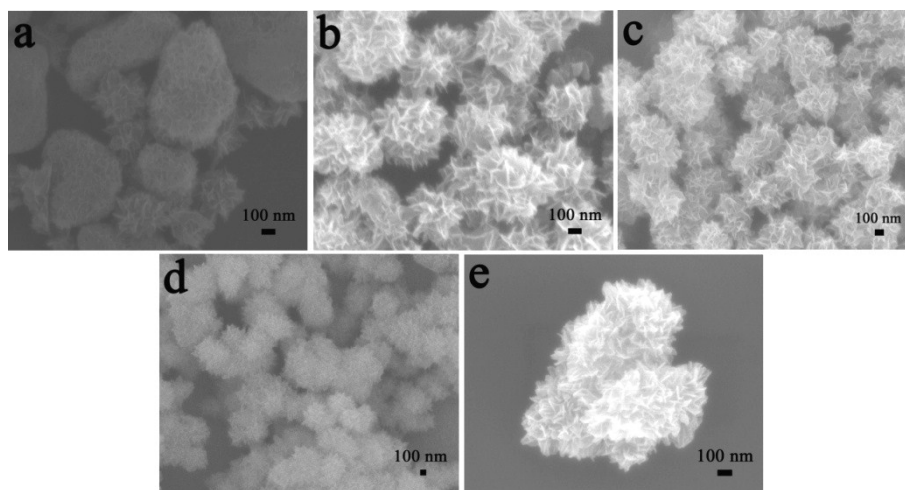


Figure S6 SEM images of γ -AlOOH@C precursor at different reaction time a) 0.5, b) 1, c) 3, d) 5 and e) 6 h (other conditions: 0.2 g Al and 3.6 g glucose, 180°C)

Figure S6 shows the typical SEM images of γ -AlOOH@C precursor prepared at different reaction times. After 0.5 h, lots of large sized ellipsoidal and subsphaeroidal structures with nanoflakes-aggregated surface began to appear (Figure S6a). An increase of the reaction time to 1.0 h initiated the dissolution process of those ellipsoidal and subsphaeroidal structures to achieve a minimum total surface free energy, and thus the flower-like structures started to form slowly by the gradually decomposition (Figure S6b). Also, it can be observed that the folds between these nanoflakes of the surface become much more obvious. Similar flower-like structures were formed after the reaction time extended to 3 h (Figure S6c), and it is worth mentioning that the flower-like structures became much more uniform. When the reaction time was increased to 5 h (Figure S6d), the flower-like structures can still be obtained. However, these structures possessed fuzzier and less obvious fold surface which may be contribute to the increased coated carbon layer thickness as the extending of reaction time. A subsequent increase of reaction time to 6.0 h caused a complete disappearance of the flower-like structure (Figure S6e), and only large

irregular aggregates consisted of a large quantity of nanoflakes were remained which can be explained by the Ostwald Ripening theory.

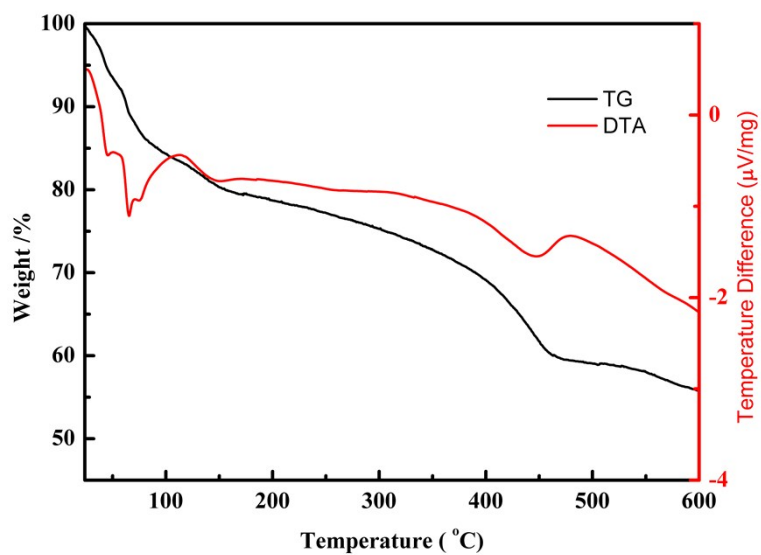


Figure S7 TG/DTA curves of γ -ALOOH performed under Ar atmosphere to investigate the crystallization of γ -ALOOH to γ -Al₂O₃.

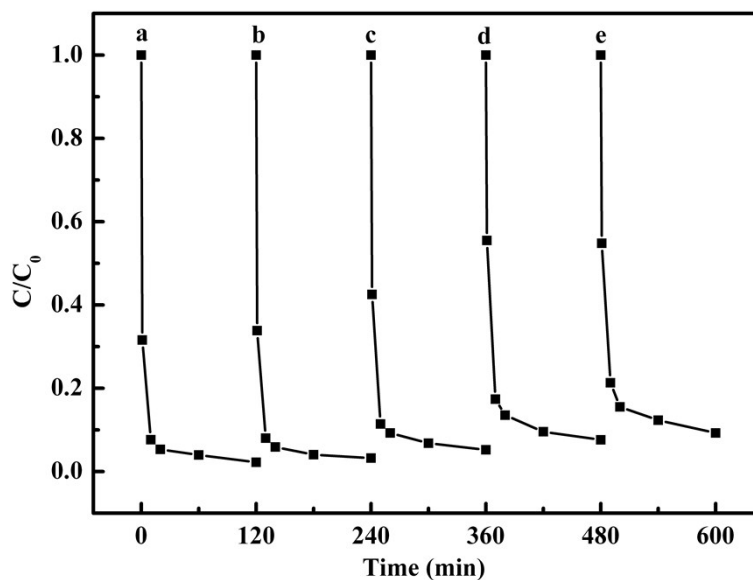


Figure S8 Adsorption rate of CR using γ -Al₂O₃@C after the (a) original adsorption, and (b) first, (c) second, (d) third, (e) fourth cycle.

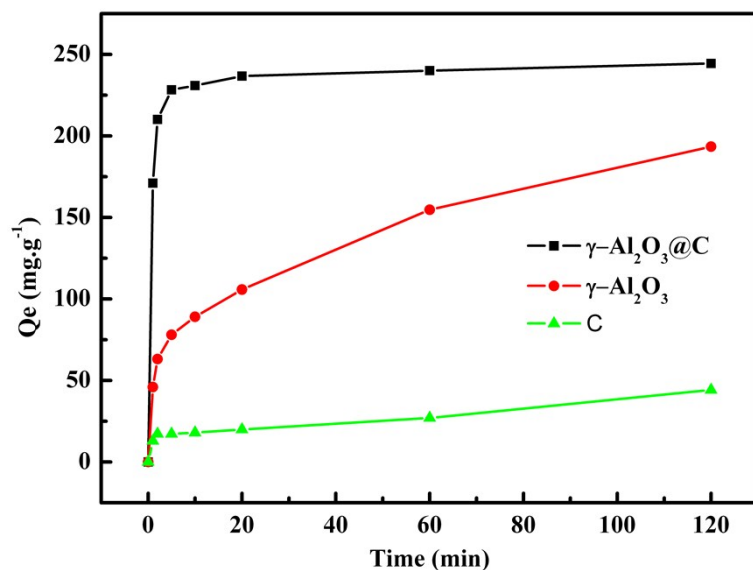


Figure S9 Time-dependent adsorption capacities of CR using $\gamma\text{-Al}_2\text{O}_3\text{@C}$, pure $\gamma\text{-Al}_2\text{O}_3$ sample obtained from $\gamma\text{-AlOOH}$ in the absence of glucose, and carbon sample obtained in the absence of Al nanopowder followed by calcinations, respectively.

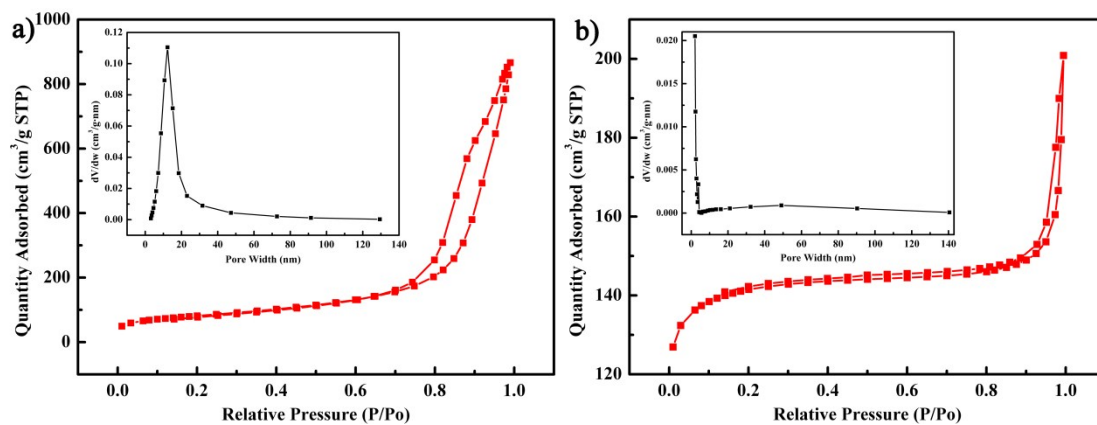


Figure S10 Nitrogen adsorption/desorption isotherm and corresponding Barrett-Joyner-Halenda (BJH) pore size distribution plot (inset) of a) $\gamma\text{-Al}_2\text{O}_3$ sample and b) carbon sample.

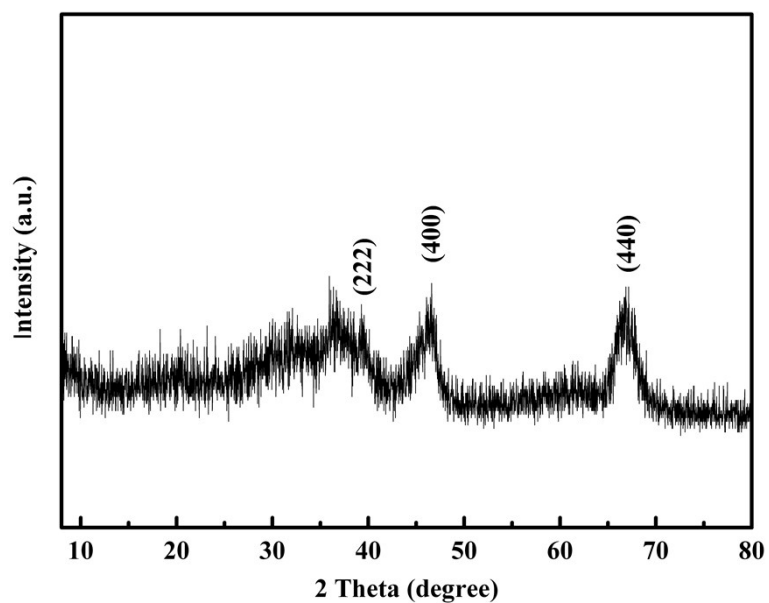


Figure S11 XRD pattern of γ - Al_2O_3 prepared from γ - AlOOH precursor.

Figure S11 shows the XRD pattern of γ - Al_2O_3 prepared from γ - AlOOH precursor. The observed diffraction peaks appear at 39.49, 45.86 and 67.03 represent (222), (400) and (440) reflections of γ - Al_2O_3 (JCPDS card No. 10-0425), respectively.

Table S1 Adsorption capacities of CR on various γ -AlOOH and γ -Al₂O₃ adsorbents.

| Type of adsorbent | Q_e (mg•g ⁻¹) | T (min) | References |
|--|-----------------------------|---------|------------|
| Mesoporous γ -Al ₂ O ₃ powders | 99.9 | 30 | [1] |
| Self-Assembled 3D Hierarchically Structured γ -Al ₂ O ₃ | 99.9 | 10 | [2] |
| 3D hierarchical γ -AlOOH hollow microspheres | 114.7 | 10 | [3] |
| γ -AlOOH hollow core/shell microspheres | 111.3 | 15 | [4] |
| SiO ₂ @ γ -AlOOH core/sheath fiber membrane | 24.3 | 90 | [5] |
| Core/shell γ -AlOOH microspheres | 31.25 | 5 | [6] |
| Flower-liked γ -Al ₂ O ₃ @C composite | 244.5 | 5 | This study |

T (min) is the corresponding adsorption time when the adsorption rate reached above 90%.

Table S2 Adsorption abilities for CR of three products.

| Absorbent samples | Adsorption capacity(mg•g ⁻¹) for CR at 5 min | Adsorption rate(%) for CR at 5 min | Adsorption capacity(mg•g ⁻¹)for CR at 120 min | Adsorption rate(%) for CR at 120 min |
|---|--|------------------------------------|---|--------------------------------------|
| γ -Al ₂ O ₃ @C | 228.3 | 91.3 | 244.5 | 97.8 |
| γ -Al ₂ O ₃ | 78.0 | 31.2 | 193.4 | 77.4 |
| C | 17.2 | 6.9 | 44.2 | 17.7 |

Table S3 The BET surface area ($\text{m}^2 \text{g}^{-1}$) and pore volume ($\text{cm}^3 \cdot \text{g}^{-1}$) of $\gamma\text{-Al}_2\text{O}_3@\text{C}$, $\gamma\text{-Al}_2\text{O}_3$, and C samples obtained from the N_2 adsorption analysis.

| Absorbent samples | $\gamma\text{-Al}_2\text{O}_3@\text{C}$ | $\gamma\text{-Al}_2\text{O}_3$ | C |
|---|---|--------------------------------|-------|
| BET surface area ($\text{m}^2 \text{g}^{-1}$) | 346.2 | 282.2 | 426.5 |
| pore volume ($\text{cm}^3 \cdot \text{g}^{-1}$) | 0.68 | 1.16 | 0.25 |

References

- [1] S. Ghosh, M.K. Naskar, Solvothermal Conversion of Nanofiber to Nanorod-Like Mesoporous $\gamma\text{-Al}_2\text{O}_3$ Powders, and Study Their Adsorption Efficiency for Congo Red, *Journal of the American Ceramic Society*, 96 (2013) 1698-1701.
- [2] Y. Li, C. Peng, L. Li, P. Rao, Self-Assembled 3D Hierarchically Structured Gamma Alumina by Hydrothermal Method, *Journal of the American Ceramic Society*, 97 (2014) 35-39.
- [3] W. Cai, S. Chen, J. Yu, Y. Hu, C. Dang, S. Ma, Template-free solvothermal synthesis of hierarchical boehmite hollow microspheres with strong affinity toward organic pollutants in water, *Materials Chemistry and Physics*, 138 (2013) 167-173.
- [4] W. Cai, J. Yu, B.L. Su, and M. Jaroniec, Synthesis of Boehmite Hollow Core Shell and Hollow Microspheres via Sodium Tartrate-Mediated Phase Transformation and Their Enhanced Adsorption Performance in Water Treatment, *J. Phys. Chem. C*, 113 (2009) 14739-14746.
- [5] Y.E. Miao, R. Wang, D. Chen, Z. Liu, T. Liu, Electrospun self-standing membrane of hierarchical $\text{SiO}_2@\gamma\text{-AlOOH}$ (boehmite) core/sheath fibers for water remediation, *ACS applied materials & interfaces*, 4 (2012) 5353-5359.
- [6] L. Zhang, W. Lu, L. Yan, Y. Feng, X. Bao, J. Ni, X. Shang, Y. Lv, Hydrothermal synthesis and characterization of core/shell AlOOH microspheres, *Microporous and Mesoporous Materials*, 119 (2009) 208-216.